Anderson localization in an ac-driven two-band model

1996 J. Phys.: Condens. Matter 8 1193

(http://iopscience.iop.org/0953-8984/8/9/010)

J. Phys.: Condens. Matter **8** (1996) 1193–1206. Printed in the UK

Anderson localization in an ac-driven two-band model

Klaus Drese and Martin Holthaus

Fachbereich Physik der Philipps-Universität, Renthof 6, D-35032 Marburg, Germany

Received 16 November 1995

Abstract. The introduction of quasienergy bands for lattices interacting with combined ac and dc fields allows us to describe the time evolution in close analogy to the field-free case. We show how such bands emerge for a two-band tight-binding model, and present analytical and numerical results for its quasienergy band structure. The ratio of disorder strength and quasienergy band width determines the localization lengths of the quasienergy states. Since the quasienergy band widths depend on the field parameters, this leads to a possibility of controlling Anderson localization by adjusting the ac amplitude. It is suggested that signatures of ac-field-controlled Anderson localization can be found by examining the temperature dependency of the conductivity of terahertz-driven semiconductor superlattices, for various values of the ac amplitude.

1. Introduction

Random disorder in periodic potentials causes Anderson localization of the electronic energy eigenstates [1–4]. In one-dimensional disordered lattices, in particular, all eigenstates are localized even for arbitrarily weak disorder. The localization lengths are determined by the ratio of disorder strength and energy band width [5]. For *finite*, weakly disordered lattices the localization lengths can exceed the size of the whole lattice, so localization is negligible and the eigenstates can be regarded as effectively extended.

Semiconductor superlattices are important examples of effectively one-dimensional, finite periodic structures. These artificially grown mesoscopic systems typically consist of about 100 lattice periods, often even less, and they inevitably contain a certain amount of disorder. Usually one is interested in high-quality superlattice samples for studying, e.g., Bloch oscillations, but it is readily possible to fabricate also intentionally disordered superlattices [6], and to investigate the effects of layer thickness fluctuations on electronic transport properties.

For a systematic experimental study of localization effects in superlattices, it would be desirable to manipulate the localization lengths within an individual sample. One could then explore the crossover effects that occur when the localization lengths are comparable to the sample size. However, since both the amount of disorder and the energy (mini-)band widths are sample-specific properties, achieving such a tunability of localization lengths appears impossible.

The situation is quite different if the superlattice is exposed to a spatially homogeneous ac electric field. Then the total Hamiltonian is periodically time dependent, and Floquet states and quasienergy bands take over the role that Bloch waves and energy bands had played in the static case [7–9]. The widths of the quasienergy bands depend strongly on the ac amplitude, and can even approach zero under certain conditions. In the presence of

0953-8984/96/091193+14$19.50

ac fields, it is the ratio of disorder strength and the amplitude-dependent *quasi*energy band width that determines the degree of localization [10–12]. Hence, in principle it is possible to change the localization lengths by suitably adjusting the amplitude of the ac field.

In this paper we extend the previous theoretical studies on ac-field-controlled Anderson localization [10–12] to include interband effects. To this end, we explore the dynamics of a single electron in a two-band tight-binding model [9, 13] driven simultaneously by a static and a resonant, oscillating field. Needless to say, this simple model cannot give a one-to-one description of all processes in real superlattices. For example, an electron in a semiconductor never experiences only the external field; it also experiences a field from induced polarization [14]. However, it has been shown recently by Meier *et al* [15–17] that consequences of the band collapse found in the ideal single-band tight-binding model [7], such as dynamic localization [18–20], survive even in the presence of Coulomb interactions, and should be experimentally observable. We may therefore assume that the idealized tight-binding model still captures a significant part of the physics of real superlattice samples. In any case, this model provides a paradigmatically clear example for the influence of interband effects on Anderson localization in ac fields. Since successful experiments with semiconductor superlattices in strong terahertz fields have already been carried out [21–24], it might be of interest to search for signatures of ac-field-controlled Anderson localization in these systems.

Our paper is organized as follows: section 2 contains a brief description of the model, as well as analytical and numerical results for its quasienergy band structure in the absence of disorder. Since the numerical computation of quasienergy bands is a straightforward matter, particular emphasis is put on a transparent explanation of the physics that leads to the emergence of these bands. Section 3 then discusses the relation between quasienergy band width and localization in the randomly disordered model, and typical effects caused by interband transitions. Some conclusions are drawn in the final part, section 4.

2. Quasienergy bands for the ideal two-band model

We consider the standard two-band tight-binding Hamiltonian for a lattice electron driven by an electric field [9, 13]:

$$H(t) = H_{0,1} + H_{F,1}(t) + H_{0,2} + H_{F,2}(t) + H_{IB}(t). \tag{1}$$

For either $j = 1$ or $j = 2$ the Hamiltonian $H_{0,j}$ describes the dynamics within a single band of width Δ_j,

$$H_{0,j} = (-1)^j \frac{D}{2} \sum_{\ell} |\ell, j\rangle\langle \ell, j| + (-1)^j \frac{\Delta_j}{4} \sum_{\ell} (|\ell+1, j\rangle\langle \ell, j| + |\ell, j\rangle\langle \ell+1, j|) \tag{2}$$

and $H_{F,j}(t)$ models the interaction with an external electric field $F(t)$:

$$H_{F,j}(t) = eF(t)d \sum_{\ell} |\ell, j\rangle \ell \langle \ell, j|. \tag{3}$$

The centres of the two unperturbed bands are separated by the energy distance D. The interaction between them is given by $H_{IB}(t)$:

$$H_{IB}(t) = eF(t)X \sum_{\ell} (|\ell, 1\rangle\langle \ell, 2| + |\ell, 2\rangle\langle \ell, 1|)\,. \tag{4}$$

We have denoted the Wannier state at the ℓth site in the jth band ($j = 1, 2$) by $|\ell, j\rangle$; e is the electronic charge, d the lattice constant, and X the interband matrix element. The

electric field consists of a static part of strength F_0 and an oscillating part with amplitude F_1 and frequency ω:

$$F(t) = F_0 + F_1 \cos(\omega t). \tag{5}$$

Throughout this paper, we adopt a system of units with $\hbar = 1$.

If the ac amplitude F_1 vanishes, then the energy spectrum of the dc-driven two-band model consists of two interspaced Wannier–Stark ladders, i.e., of two sequences of energy eigenvalues with constant spacing $\Delta E = eF_0 d$ between adjacent members of each sequence [13].

On the other hand, if the amplitude F_1 of the ac field is so high that standard low-order perturbation theory ceases to be applicable, it is no longer practical to analyse the dynamics in terms of energy eigenstates and energy eigenvalues. Rather, one can resort to Floquet theory: given a quantum system governed by a Hamiltonian $H(t)$ that is periodic in time, with period $T = 2\pi/\omega$, there should be a complete set $\{\psi_r(t)\}$ of solutions to the Schrödinger equation $\mathrm{i}\,\partial_t \psi(t) = H(t)\psi(t)$ of the particular form [25, 26]

$$\psi_r(t) = u_r(t) \exp(-\mathrm{i}\varepsilon_r t) \tag{6}$$

where the functions $u_r(t)$ inherit the T-periodicity of the Hamiltonian:

$$u_r(t) = u_r(t + T). \tag{7}$$

A wave function $\psi_r(t)$ is called Floquet state, with quasienergy ε_r. Inserting such a Floquet state into the Schrödinger equation, one obtains

$$[H(t) - \mathrm{i}\,\partial_t]\, u_r(t) = \varepsilon_r u_r(t). \tag{8}$$

Hence, the periodic functions $u_r(t)$ and the quasienergies ε_r can be computed by solving the eigenvalue problem associated with the operator $[H(t) - \mathrm{i}\,\partial_t]$ in an extended Hilbert space consisting of T-periodic functions [27]. The scalar product in that space

$$\langle\langle \cdot \,|\, \cdot \rangle\rangle \;:=\; \frac{1}{T} \int_0^T \mathrm{d}t \;\; \langle \cdot \,|\, \cdot \rangle \tag{9}$$

is the usual scalar product combined with time averaging. The conceptual advantage of the Floquet states lies in the fact that an arbitrary solution $\psi(t)$ to the Schrödinger equation can be expanded as

$$\psi(t) = \sum_r a_r u_r(t) \exp(-\mathrm{i}\varepsilon_r t) \tag{10}$$

with time-independent coefficients a_r.

Exactly as a quasimomentum in a periodic lattice is defined up to an integer multiple of the reciprocal-lattice vector, a quasienergy is defined up to an integer multiple of ω: if $u_r(t)$ is a T-periodic solution to the eigenvalue equation (8) with quasienergy ε_r, and if m is an arbitrary, positive or negative integer, then also $u_r(t)\exp(\mathrm{i}m\omega t)$ is a T-periodic eigensolution, with quasienergy $\varepsilon_r + m\omega$. All of these replicas are physically equivalent, because

$$u_r(t) \exp(\mathrm{i}m\omega t) \exp(-\mathrm{i}[\varepsilon_r + m\omega]t) = u_r(t) \exp(-\mathrm{i}\varepsilon_r t). \tag{11}$$

Nevertheless, *all* solutions to (8) are required for the completeness relation in the extended Hilbert space.

If one applies this Floquet theory to the lattice Hamiltonian (1), one accounts for the T-periodicity induced by the ac field. It must be recognized, however, that the dc field also induces time-periodic wave-packet motion, that is, Bloch oscillations [28]. If the Bloch frequency $\omega_{Bloch} = eF_0 d$ is different from the ac frequency ω, then the Floquet states,

which mark out *one* type of periodicity, might not provide the optimal basis. The problem becomes obvious on changing the gauge: the Hamiltonian (1) is unitarily equivalent to

$$\begin{aligned}\widetilde{H}(t) = &\sum_{j=1,2}\sum_{\ell}(-1)^j\frac{D}{2}|\ell,\,j\rangle\langle\ell,\,j| \\ &+\sum_{j=1,2}\sum_{\ell}(-1)^j\frac{\Delta_j}{4}\left(\mathrm{e}^{-\mathrm{i}eA(t)d}|\ell+1,\,j\rangle\langle\ell,\,j| + |\ell,\,j\rangle\langle\ell+1,\,j|\mathrm{e}^{+\mathrm{i}eA(t)d}\right) \\ &+eF(t)X\sum_{\ell}\left(|\ell,1\rangle\langle\ell,2| + |\ell,2\rangle\langle\ell,1|\right) \qquad (12)\end{aligned}$$

where

$$A(t) = -F_0 t - \frac{F_1}{\omega}\sin(\omega t) \qquad (13)$$

is the gauge potential. Unless the Bloch frequency $\omega_{Bloch} = eF_0 d$ and the ac frequency ω are rationally related, the phase factors $\exp(\pm\mathrm{i}eA(t)d)$ are quasiperiodic functions of time. In order to account for this type of time dependence, one should apply two-mode Floquet theory to $\widetilde{H}(t)$. There is, however, an important case where T-periodicity is not affected by the gauge transformation: if ω_{Bloch} is a multiple of ω, then both (1) and (12) are T-periodic, and the Floquet states can incorporate the effects of both the ac and the dc field in an optimal way.

With this caveat in mind, we now turn to the eigenvalue problem (8) for the two-band tight-binding Hamiltonian (1). We proceed in several steps. First we rewrite $H(t)$ as

$$H(t) = H_0 + \sum_{\ell}H_{IB}^{(\ell)}(t) + \sum_{\ell}H_F^{(\ell)}(t) \qquad (14)$$

where

$$H_0 = H_{0,1} + H_{0,2} \qquad (15)$$

is the time-independent part. Field-induced transitions between the two Wannier states at the ℓth site are described by

$$H_{IB}^{(\ell)}(t) = \left(|\ell,2\rangle\langle\ell,1| + |\ell,1\rangle\langle\ell,2|\right)eX(F_0 + F_1\cos(\omega t)) \qquad (16)$$

and

$$H_F^{(\ell)}(t) = \left(|\ell,1\rangle\langle\ell,1| + |\ell,2\rangle\langle\ell,2|\right)e\ell d(F_0 + F_1\cos(\omega t)) \qquad (17)$$

is the diagonal part of the interaction with the electric field. In order to compute the quasienergy bands for the model (1), i.e., the spectrum of $[H(t) - \mathrm{i}\,\partial_t]$, we will first derive the exact Floquet states for the operator $[H(t) - H_0 - \mathrm{i}\,\partial_t]$, and then treat H_0 perturbatively.

Solutions to the Schrödinger equations

$$\left[H_{IB}^{(\ell)}(t) + H_F^{(\ell)}(t) - \mathrm{i}\,\partial_t\right]\varphi^{(\ell)}(t) = 0 \qquad (18)$$

are given by

$$\varphi_{\pm}^{(\ell)}(t) = \frac{1}{\sqrt{2}}\left(|\ell,1\rangle \pm |\ell,2\rangle\right)\exp\left(-\mathrm{i}(\pm eX + e\ell d)\left(F_0 t + F_1\frac{\sin(\omega t)}{\omega}\right)\right). \qquad (19)$$

Evidently, these are Floquet states with quasienergies

$$\varepsilon_{\pm}^{(\ell)} = \pm eF_0 X + \ell eF_0 d \qquad \mathrm{mod}\ \omega. \qquad (20)$$

The individual on-site Floquet states $\varphi_{\pm}^{(\ell)}(t)$ are coupled by the hopping terms in H_0. They can hybridize and form quasienergy bands of finite width *only* if they are quasienergetically degenerate with their nearest neighbours—i.e., if there exists an integer n such that

$$eF_0 d = n\omega. \tag{21}$$

This condition for quasienergetic alignment simply means that the energy of n photons matches the energy difference between adjacent rungs of the Wannier–Stark ladders. As noted before, this is also the condition for the Floquet states to constitute an optimal basis. In the following we will therefore assume that the ac frequency is tuned such that (21) is satisfied.

We then form linear superpositions

$$\psi_{\pm}(k;t) = \sum_{\ell} \exp(-\mathrm{i}k\ell d)\varphi_{\pm}^{(\ell)}(t) \equiv u_{\pm}(k;t)\exp(-\mathrm{i}\varepsilon_{\pm}t). \tag{22}$$

By construction, the T-periodic functions $u_{\pm}(k;t)$:

$$u_{\pm}(k;t) = \frac{1}{\sqrt{2}}\sum_{\ell}(|\ell,1\rangle \pm |\ell,2\rangle)\exp\left(-\mathrm{i}k\ell d - \mathrm{i}\ell n\omega t - \mathrm{i}(\ell d \pm X)\frac{eF_1}{\omega}\sin(\omega t)\right) \tag{23}$$

are extended quasienergy eigenfunctions of the operator $[H(t) - H_0 - \mathrm{i}\,\partial_t]$, provided that (21) holds. Their quasienergy eigenvalues, $\varepsilon_{\pm} = \pm eF_0 X \bmod \omega$, are degenerate with respect to the wave vector k.

In general, this degeneracy will be removed as a consequence of the hopping between nearest neighbours as described by H_0. If both the hopping strengths and the unperturbed energy band separation are small, i.e., if $\Delta_1/\omega \ll 1$, $\Delta_2/\omega \ll 1$, and $D/\omega \ll 1$, we can treat the effect of H_0 on the spectrum by low-order perturbation theory in the extended Hilbert space [27]. Since H_0 has nonvanishing matrix elements only between Floquet eigenfunctions (23) that are characterized by the same wave vector, k is a good quantum number. We have to distinguish two cases: if there is no integer m such that

$$2eF_0 X = m\omega \tag{24}$$

then ε_+ and ε_- do not coincide (mod ω), and we can resort to nondegenerate perturbation theory. Since

$$\langle u_{\pm}(k';t)|H_0|u_{\pm}(k;t)\rangle = \frac{\Delta_2 - \Delta_1}{4}\cos\left(kd + n\omega t + \frac{eF_1 d}{\omega}\sin(\omega t)\right)\delta_{k,k'} \tag{25}$$

the required matrix elements in the extended Hilbert space are

$$\langle\langle u_{\pm}(k';t)|H_0|u_{\pm}(k;t)\rangle\rangle = \frac{\Delta_2 - \Delta_1}{4}J_{-n}\left(\frac{eF_1 d}{\omega}\right)\cos(kd)\,\delta_{k,k'}. \tag{26}$$

Hence, we obtain the quasienergy–quasimomentum dispersion relations

$$\varepsilon_{\pm}(k) = \pm eF_0 X + (-1)^n \frac{\Delta_2 - \Delta_1}{4}J_n\left(\frac{eF_1 d}{\omega}\right)\cos(kd) \qquad \bmod \omega. \tag{27}$$

Within this first-order approximation, the two quasienergy bands are simple cosine bands with identical widths, and they both collapse when the dimensionless ac amplitude $eF_1 d/\omega$ equals a zero $j_{n,s}$ of the ordinary Bessel function J_n, exactly as in the case of a single band [7, 8, 12].

FIG 1 a+b+c —add with macros

The approximate spectrum (27) does not contain the original energy band separation D. If D is not small compared to the ac frequency, but still $\Delta_j/\omega \ll 1$ for $j = 1, 2$, one can consider first the limiting case where $\Delta_1/\omega = \Delta_2/\omega = 0$. Then the Hamiltonian (1) still

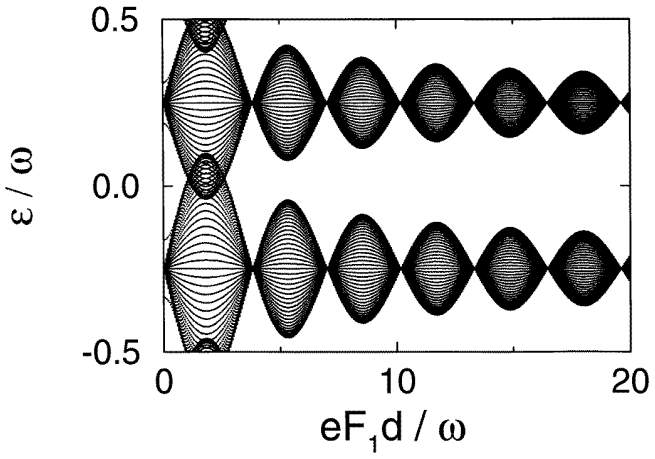

(a)

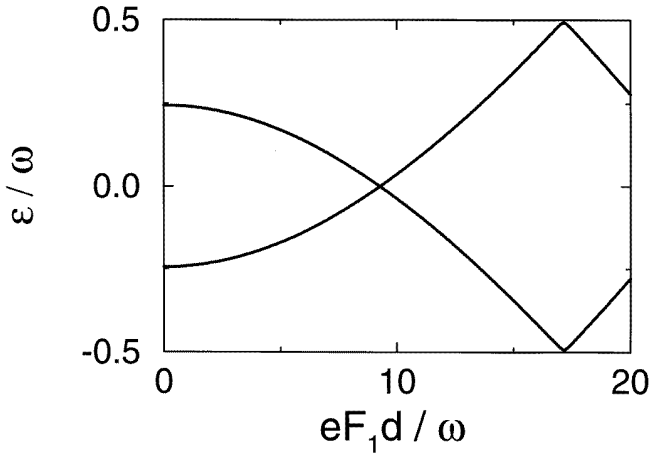

(b)

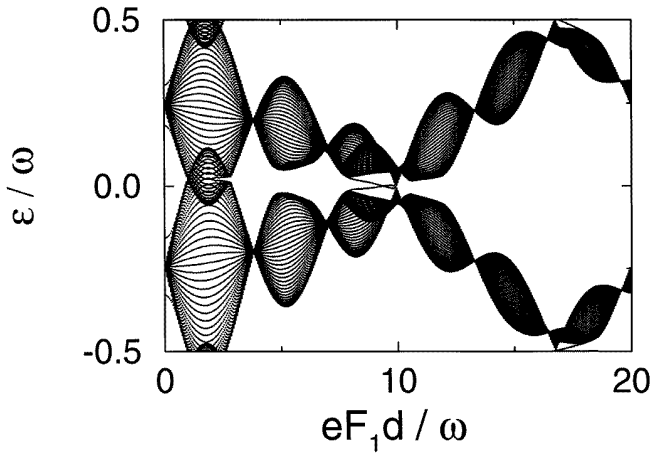

(c)

Figure 1. See facing page.

Figure 1. (See facing page.) Quasienergy bands for the two-band model (1) with 41 sites, versus the scaled ac amplitude eF_1d/ω. The case considered here is a one-photon resonance, $eF_0d = 1\omega$. (a) Vanishing interband interaction, $X/d = 0$. The energy band widths are $\Delta_1/\omega = 1.0$, $\Delta_2/\omega = 1.2$; the energy band separation is $D/\omega = 5.5$. Both quasienergy bands collapse at the zeros of J_1. (b) $X/d = -16/(9\pi^2)$, but $\Delta_j/\omega = 0$ $(j = 1, 2)$. (c) Quasienenergy bands with Δ_j/ω as in (a), and X/d as in (b). Note that the band collapses are hardly affected by the interband interaction.

reduces to a system of uncoupled two-level systems $H_{tls}^{(\ell)}(t)$ that are labelled by the site index ℓ:

$$H_{tls}^{(\ell)}(t) = \frac{D}{2}\sigma_z + eF(t)\ell d\,\mathbf{1} + eF(t)X\sigma_x \tag{28}$$

where σ_x and σ_z are the usual Pauli matrices. The quasienergy spectra of all of these systems coincide, provided that the resonance condition (21) is satisfied. If then $\Delta_1/\omega \neq 0$ and $\Delta_2/\omega \neq 0$, and so different sites communicate with each other, this ℓ-degeneracy is again removed, and quasienergy bands emerge. The centres of these bands tend to follow the quasienergies of the associated two-level systems (28), and their widths tend to oscillate proportionally to $J_n(eF_1d/\omega)$, as in the case where $D/\omega \ll 1$.

Figure 1 depicts such a scenario for a finite lattice with $N = 41$ sites; the wave functions are assumed to vanish at the chain ends. Plot (a) shows the two quasienergy bands without interaction ($X/d = 0$), versus the scaled ac amplitude eF_1d/ω. The parameters chosen are $n = 1$ (that is, we have a one-photon resonance, $eF_0d = 1\omega$), $\Delta_1/\omega = 1.0$, $\Delta_2/\omega = 1.2$, and $D/\omega = 5.5$. Plot (b) shows the quasienergies for the two-level systems (28). The value of the interband matrix element is $X/d = -16/(9\pi^2)$ [9], so the second resonance (24) is not met. Plot (c) shows the quasienergy bands for the full system, with Δ_j/ω as in (a) and X/d as in (b). The band collapses are hardly affected by the interband interaction; they occur at the same ac amplitudes as in the case where $X/d = 0$.

The quasienergy spectrum becomes more complicated if, besides the basic condition (21) required for the emergence of quasienergy bands, the second resonance condition (24) is also satisfied. Then the quasienergies $\varepsilon_{tls,\pm}^{(\ell)}$ of the two-level systems (28) show the strongest dependency on the ac amplitude. A standard calculation [29] readily yields a strong-field approximation:

$$\varepsilon_{tls,\pm}^{(\ell)} = \frac{m\omega}{2} \pm (-1)^m \frac{D}{2} J_m\left(\frac{2eF_1X}{\omega}\right) \qquad \text{mod } \omega \tag{29}$$

which shows that the already familiar Bessel function $J_n(eF_1d/\omega)$ resulting from the coupling of adjacent sites now has to compete with the Bessel function $J_m(2eF_1X/\omega)$ originating from the coupling of the two Wannier–Stark ladders.

The calculation of the approximate quasienergy band structure for the case where $\Delta_j/\omega \ll 1$ $(j = 1, 2)$, $D/\omega \ll 1$, requires degenerate perturbation theory, since, by virtue of of (24), the quasienergy eigenfunctions $u_+(k;t)$ and $u_-(k;t)\mathrm{e}^{\mathrm{i}m\omega t}$ belong to the same quasienergy. Hence, besides the matrix elements (26) we also need

$$\begin{aligned}\langle\langle u_+(k;t)|H_0|u_-(k;t)\mathrm{e}^{\mathrm{i}m\omega t}\rangle\rangle \\ = -(-1)^m \frac{D}{2} J_m\left(\frac{2eF_1X}{\omega}\right) \\ -\frac{\Delta_1+\Delta_2}{8}\left[\mathrm{e}^{\mathrm{i}kd} J_{-n-m}\left(\frac{(2X+d)eF_1}{\omega}\right) + \mathrm{e}^{-\mathrm{i}kd} J_{n-m}\left(\frac{(2X-d)eF_1}{\omega}\right)\right].\end{aligned} \tag{30}$$

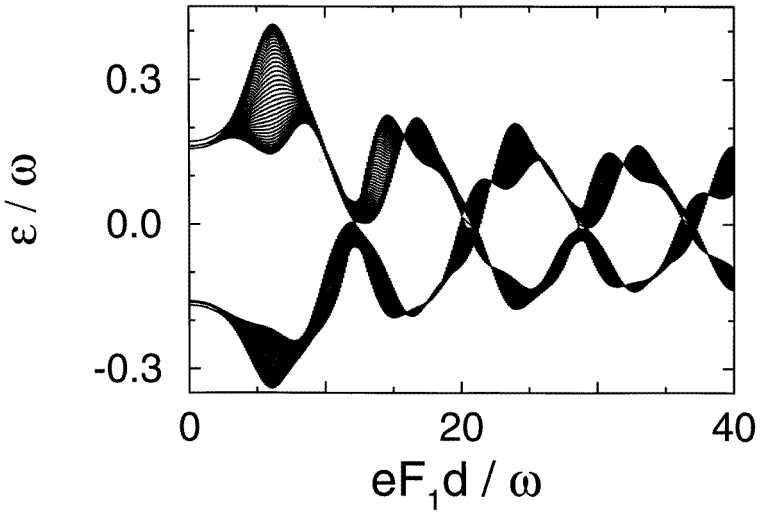

(a)

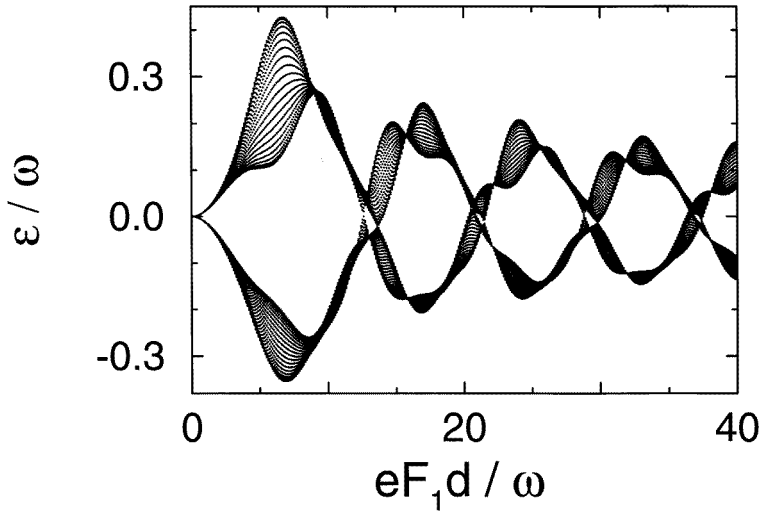

(b)

Figure 2. Quasienergy bands for a case of double resonance. (a) Numerically computed quasienergy bands for a finite lattice with 41 sites, for $n = 5$ and $m = -2$ ($X/d = -0.2$). The other parameters are $D/\omega = 1.2$, $\Delta_1/\omega = 0.4$, and $\Delta_2/\omega = 0.8$. (b) Evaluation of the approximate formula (33) for these parameters.

Defining the dimensionless parameters

$$\alpha = \frac{eF_1 d}{\omega} \tag{31}$$

and

$$\beta = \frac{2eF_1 X}{\omega} \tag{32}$$

we then obtain the approximate quasienergy bands for the case where both resonance conditions (21) and (24) are satisfied:

$$\varepsilon_{\pm}(k) = \frac{m\omega}{2} + (-1)^n \frac{\Delta_2 - \Delta_1}{4} J_n(\alpha)\cos(kd) \pm \Bigg[\frac{D^2}{4} J_m^2(\beta) + \left(\frac{\Delta_1 + \Delta_2}{8}\right)^2 \times \left(J_{m+n}^2(\beta+\alpha) + J_{m-n}^2(\beta-\alpha) + 2J_{m+n}(\beta+\alpha)J_{m-n}(\beta-\alpha)\cos(2kd)\right) + (-1)^n D \frac{\Delta_1 + \Delta_2}{8} \times J_m(\beta)\cos(kd)\left(J_{m+n}(\beta+\alpha) + J_{m-n}(\beta-\alpha)\right) \Bigg]^{1/2} \quad \text{mod } \omega. \tag{33}$$

These are no longer simple cosine bands. Depending on the respective values of the integers n and m, up to four different Bessel functions appear. The widths of the quasienergy bands still depend strongly on the ac amplitude, but there are no perfect band collapses.

Figure 2(a) depicts the numerically computed quasienergy bands for a finite lattice with 41 sites, for $\Delta_1/\omega = 0.4$, $\Delta_2/\omega = 0.8$, and $D/\omega = 1.2$. We have chosen $n = 5$ and $X/d = -0.2$, which gives $m = -2$. Figure 2(b) shows the evaluation of (33) for these parameters. Since D/ω is not really small, the approximation fails at low ac amplitudes. For high amplitudes, however, the agreement is quite good, thus indicating the correctness of our line of reasoning.

It should be pointed out that for nonvanishing dc fields both resonance conditions (21) and (24) can be satisfied simultaneously only if $2X/d = m/n$ is a ratio of two integers. Of course, any given ratio $2X/d$ could be approximated arbitrarily well by rational numbers, but the resonances will be physically meaningful only if both n and m are small. However, if there is no dc field at all, then both conditions are satisfied automatically, with $n = m = 0$. In that case the analytical formula (33) shows that the quasienergy bands no longer collapse perfectly when α equals a zero of J_0, as has recently been observed in numerical studies by Rotvig *et al* [9]. Whether or not an approximate collapse occurs depends on the values of both α and β.

3. Amplitude-controlled Anderson localization

We now introduce site-diagonal random disorder into the tight-binding model by adding to $H(t)$ the Hamiltonian

$$H_{random} = \sum_{\ell} \nu_\ell \left(|\ell, 1\rangle\langle \ell, 1| + |\ell, 2\rangle\langle \ell, 2|\right). \tag{34}$$

We assume that the random energies ν_ℓ are distributed uniformly in the interval $[-\nu_{max}, +\nu_{max}]$, and so their probability distribution $\rho(\nu)$ is given by

$$\rho(\nu) = \begin{cases} 1/(2\nu_{max}) & \text{for } |\nu| \leqslant \nu_{max} \\ 0 & \text{otherwise.} \end{cases} \tag{35}$$

Figure 3(a) shows an example for the effect of disorder on the quasienergy spectrum. The parameters chosen are the same as in figure 1(c); the disorder strength is $\nu_{max}/\omega = 0.05$.

The random disorder leads to localization of the quasienergy band states. To investigate this localization we expand the numerically computed quasienergy states $u_r(t)$ in the basis of the Wannier states:

$$u_r(t) = \sum_{\ell=1}^{N} \left(c_{\ell,1}^{(r)}(t)|\ell, 1\rangle + c_{\ell,2}^{(r)}(t)|\ell, 2\rangle \right) \tag{36}$$

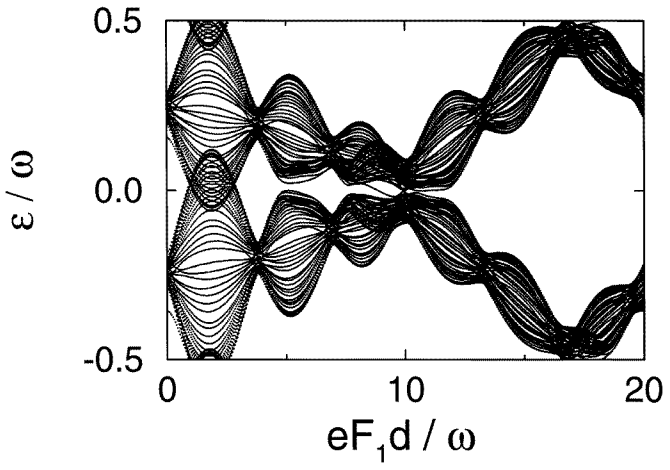

(a)

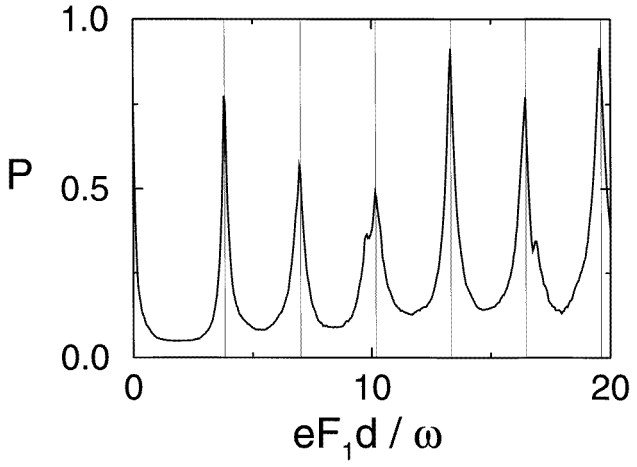

(b)

Figure 3. (a) The quasienergy spectrum for a randomly disordered two-band model with the same parameters as in figure 1(c). The disorder strength is $\nu_{max}/\omega = 0.05$. (b) The corresponding averaged inverse participation ratio P; see (38). The vertical lines indicate dimensionless amplitudes eF_1d/ω that correspond to zeros of the Bessel function J_1, where the quasienergy bands of the ideal lattice collapse.

and compute the inverse participation ratios:

$$P^{(r)}(t) = \sum_{\ell=1}^{N} \left(|c_{\ell,1}^{(r)}(t)|^2 + |c_{\ell,2}^{(r)}(t)|^2 \right)^2 . \tag{37}$$

These quantities measure the spatial extent of the quasienergy states. $P^{(r)}(t)$ approaches unity when $u_r(t)$ is localized entirely at a single site, and vanishes as N^{-1} when $u_r(t)$ is uniformly extended. The time dependence of $P^{(r)}(t)$, $r = 1, \ldots, 2N$, becomes weak when the ac frequency ω is larger than the energy band widths Δ_1 and Δ_2 [12, 30]. It then suffices to represent the functions $P^{(r)}(t)$ by their values at some arbitrary moment t_0. For

numerical convenience we choose $t_0 = 3T/4$, where the ac field vanishes. However, this particular choice is without major significance for the results that follow.

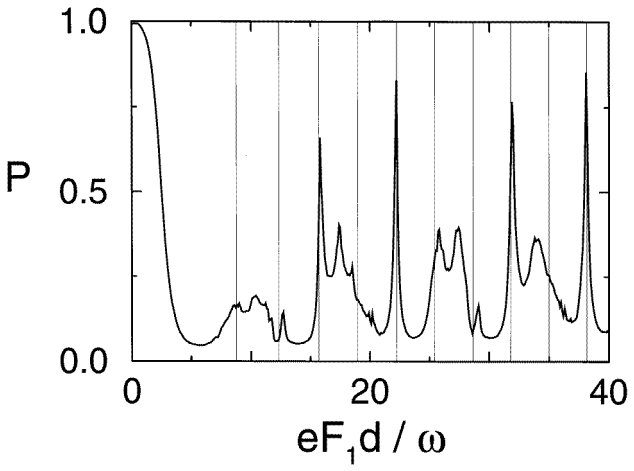

Figure 4. The inverse participation ratio for the model with the same parameters as in figure 2(a), and additional disorder of strength $\nu_{max}/\omega = 0.01$. The vertical lines indicate zeros of J_5.

A measure for the degree of disorder-induced localization is now the averaged inverse participation ratio

$$P := \frac{1}{2N}\sum_{r=1}^{2N} P^{(r)}(3T/4). \tag{38}$$

Figure 3(b) shows P as function of the scaled ac amplitude eF_1d/ω for the situation considered in figure 3(a). Localization is most strongly pronounced at the zeros of J_1, where the widths of the quasienergy bands are minimal, and comparatively weak in between. This result is not trivial. The Hamiltonian $H(t)$ for the ideal lattice describes Bloch oscillations, Zener tunnelling, and Rabi oscillations between the unperturbed energy bands. The quasienergy band states that reflect the dynamics in resonant ac fields incorporate these phenomena. Nevertheless, in the presence of disorder they behave just like energy band states in the static case: the degree of localization is determined by the ratio of disorder strength and band width. Since now the band widths depend on the ac amplitude, changing the amplitude means changing the localization lengths.

The situation studied in figure 3 is still comparatively simple, since the second resonance condition (24) is not met, and the behaviour of the two bands is not too different from that in the noninteracting case ($X/d = 0$). If (24) is satisfied, the dynamics is richer and, as a consequence, the dependency of P on the ac amplitude more complicated. We display in figure 4 the averaged inverse participation ratio for such a situation. The system parameters are as in figure 2(a), and there is additional disorder of strength $\nu_{max}/\omega = 0.01$ (so $\nu_{max}/\Delta_1 = 0.025$, $\nu_{max}/\Delta_2 = 0.0125$). Since we now have a five-photon resonance between the rungs of the Wannier–Stark ladders, vertical lines are drawn to indicate the zeros of J_5. There is still pronounced localization at *some* of the zeros, but the fluctuations of P between the spikes are apparently unrelated to the other zeros. A glance at figure 2(a) shows the reason for this: the two quasienergy bands exhibit avoided crossings when $2eF_1X/\omega$ is approximately equal to a zero of J_2. Then the single-band dynamics is strongly modified,

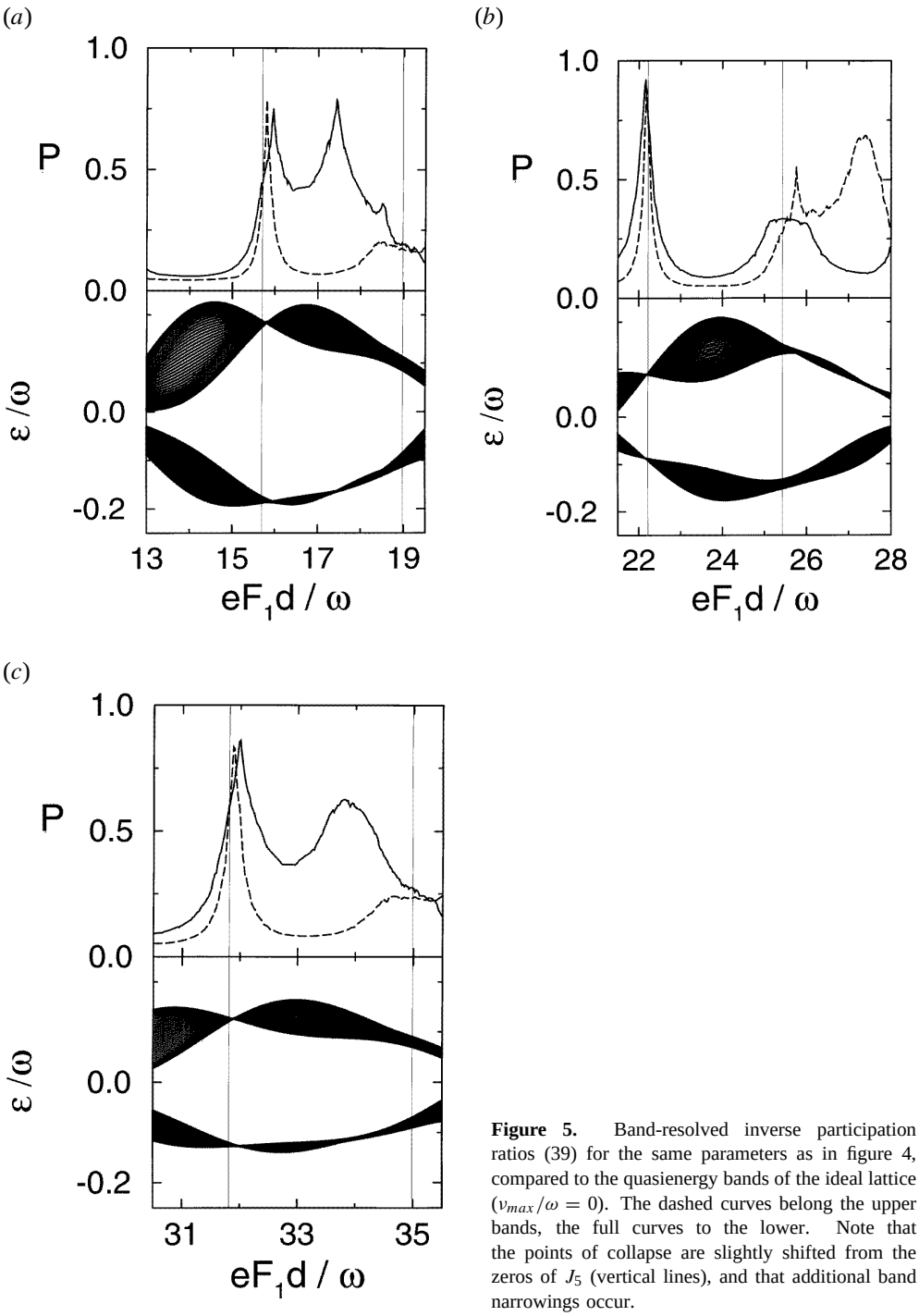

Figure 5. Band-resolved inverse participation ratios (39) for the same parameters as in figure 4, compared to the quasienergy bands of the ideal lattice ($v_{max}/\omega = 0$). The dashed curves belong the upper bands, the full curves to the lower. Note that the points of collapse are slightly shifted from the zeros of J_5 (vertical lines), and that additional band narrowings occur.

and the band widths do not follow the simple J_5-pattern. The actual connection between quasienergy band width and degree of localization, however, remains valid.

To further substantiate this statement, we also compute the band-resolved participation ratios

$$P_{br} := \frac{1}{N} \sum_{\text{one band}} P^{(r)}(3T/4) \tag{39}$$

where the summation extends only over indices r pertaining to one of the two quasienergy bands. The upper parts of figures 5(a), 5(b), and 5(c) show results of such calculations; the lower parts depict the corresponding quasienergy bands for the *ideal* model ($\nu_{max}/\omega = 0$). The parameters are as in figure 4. In all three cases, the dashed curve belongs to the upper band and the full curve to the lower one; vertical lines are drawn at zeros of J_5. The behaviour of P_{br} reflects even fine details visible in the quasienergy bands, such as slight shifts of the collapse points away from the zeros of J_5, and the appearance of additional band narrowings in only one of the bands.

4. Conclusions

The original energy bands of the two-band model are coupled by Rabi oscillations and Zener tunnelling. An arbitrary wave packet, initially prepared in one of the bands, will soon acquire components in the other. The introduction of quasienergy states corresponds to a transformation from these interacting bands to *noninteracting* quasienergy bands: a wave packet can be characterized by its expansion coefficients with respect to the quasienergy states, and these coefficients remain constant in time; see (10). Since the quasienergy states already incorporate both the ac and the dc field, they serve as a basis which allows us to describe the time evolution in complete analogy to the field-free case.

It is remarkable that this analogy extends even further. When there is random lattice disorder, the quasienergy band states localize in space. The dimensionless parameter that determines the degree of localization is the ratio of disorder strength and band width, exactly as in the well known case of Anderson localization of energy eigenstates in random lattices without external fields. But now there is an important new feature: the quasienergy bands reflect both the spatial lattice periodicity and the temporal periodicity induced by the driving fields. Varying the amplitude of the ac field means changing the properties of the spatio-temporal lattice, and, hence, changing its quasienergy band structure. For disordered lattices, varying the band widths means controlling the degree of localization. In principle, therefore, there exists a possibility of controlling Anderson localization with spatially homogeneous ac fields.

Even though there is still a long way to go from our idealized model to an actual superlattice sample, it is tempting to speculate about possible implications of the results outlined in this paper for current experiments that probe the dynamics of semiconductor superlattices under the influence of strong terahertz radiation [21–24]. For parameters where the quasienergy bands are sufficiently wide, the inevitable disorder in these mesoscopic systems might play only a minor role, so electronic transport should proceed via the effectively extended states. In that case, phonon scattering would *impede* the flow of electrons. On the other hand, there exist only localized states at field parameters where the quasienergy bands (almost) collapse, so phonon scattering would now be a mechanism that *helps* the electrons to hop from one site to another. That could result in a conductivity that *decreases* with temperature when the quasienergy bands are wide, but *increases* with temperature when they are collapsed. The observation of a strongly amplitude-dependent conductivity–temperature relation would, therefore, be an indication for Anderson localization of quasienergy states. It might also be attractive to perform experiments with

intentionally disordered superlattices. In any case, the further exploration of the concept of ac-field-controlled Anderson localization presents a new challenge to both theorists and experimentalists.

Acknowledgments

MH wishes to thank DW Hone for many fruitful discussions. This work was partially supported by the Deutsche Forschungsgemeinschaft under grant No HO 1771/1-1.

References

[1] Anderson P W 1958 *Phys. Rev.* **109** 1492
[2] Mott N F and Twose W D 1961 *Adv. Phys.* **10** 107
[3] Thouless D J 1974 *Phys. Rep.* **13** 93
[4] Kramer B and MacKinnon A 1993 *Rep. Prog. Phys.* **56** 1469
[5] Thouless D J 1979 *Ill-Condensed Matter: Les Houches Session XXXI* ed R Balian, R Maynard and G Toulouse (Amsterdam: North-Holland)
[6] Mäder K A, Wang L-W and Zunger A 1995 *Phys. Rev. Lett.* **74** 2555
[7] Holthaus M 1992 *Phys. Rev. Lett.* **69** 351
[8] Zak J 1993 *Phys. Rev. Lett.* **71** 2623
[9] Rotvig J, Jauho A-P and Smith H 1995 *Phys. Rev. Lett.* **74** 1831
[10] Holthaus M, Ristow G H and Hone D W 1995 *Phys. Rev. Lett.* **75** 3914
[11] Holthaus M, Ristow G H and Hone D W 1995 *Europhys. Lett.* **32** 241
[12] For a review, see
Holthaus M and Hone D W 1995 Localization effects in ac-driven tight-binding lattices *Preprint* NSF-ITP-95-125 (Marburg/Santa Barbara, CA)
[13] Fukuyama H, Bari R A and Fogedby H C 1973 *Phys. Rev.* B **8** 5579
[14] Büttiker M 1993 *J. Phys.: Condens. Matter* **5** 9361
[15] Meier T, von Plessen G, Thomas P and Koch S W 1994 *Phys. Rev. Lett.* **73** 902
[16] Meier T, von Plessen G, Thomas P and Koch S W 1995 *Phys. Rev.* B **51** 14 490
[17] Meier T, Rossi F, Thomas P and Koch S W 1995 *Phys. Rev. Lett.* **75** 2558
[18] Dunlap D H and Kenkre V M 1986 *Phys. Rev.* B **34** 3625
[19] Hong Shon N and Nazareno H N 1992 *J. Phys.: Condens. Matter* **4** L611
[20] Ignatov A A, Schomburg E, Grenzer J, Renk K F and Dodin E P 1995 *Z. Phys.* B **98** 187
[21] Guimarães P S S, Keay B J, Kaminski J P, Allen S J, Hopkins P F, Gossard A C, Florez L T and Harbison J P 1993 *Phys. Rev. Lett.* **70** 3792
[22] Ignatov A A, Schomburg E, Renk K F, Schatz W, Palmier J F and Mollot F 1994 *Ann. Phys., Lpz.* **3** 137
[23] Keay B J, Allen S J, Galán J, Kaminsky J P, Campman K L, Gossard A C, Bhattacharya U and Rodwell M J W 1995 *Phys. Rev. Lett.* **75** 4098
[24] Keay B J, Zeuner S, Allen S J, Maranowski K D, Gossard A C, Bhattacharya U and Rodwell M J W 1995 *Phys. Rev. Lett.* **75** 4102
[25] Zel'dovich Ya B 1966 *Zh. Eksp. Teor. Fiz.* **51** 1492 (Engl. Transl. 1967 *Sov. Phys.–JETP* **24** 1006)
[26] Ritus V I 1966 *Zh. Eksp. Teor. Fiz.* **51** 1544 (Engl. Transl. 1967 *Sov. Phys.–JETP* **24** 1041)
[27] Sambe H 1973 *Phys. Rev.* A **7** 2203
[28] Zener C 1934 *Proc. R. Soc.* A **145** 523
[29] Shirley J H 1965 *Phys. Rev.* **138** B979
[30] Hone D W and Holthaus M 1993 *Phys. Rev.* B **48** 15 123